Tumor Biol. (2016) 37:201–209
DOI 10.1007/s13277-015-3687-5

RESEARCH ARTICLE

MiR-491 attenuates cancer stem cells-like properties of hepatocellular carcinoma by inhibition of GIT-1/NF-κB-mediated EMT

Xiaojun Yang[1] · Jing Ye[1] · Han Yan[1] · Zhaoyang Tang[1] · Jian Shen[1] · Jianping Zhang[1] · Lihua Yang[2]

Received: 6 April 2015 / Accepted: 17 June 2015 / Published online: 19 July 2015

Abstract Hepatocellular carcinoma (HCC) is the most common liver malignancy. Current standard practices for treatment of HCC are less than satisfactory because of CSCs-mediated recurrence. For this reason, targeting CSCs, or cancer cells with CSCs-like properties, is a new approach for HCC treatment. As we reported previously, microRNA-491 (miR-491) is lower expressed in poorly differentiated HCC tissues relative to well-differentiated HCC tissues. Here, we further evaluate the effects of miR-491 on the CSCs-like properties by using HCC cell lines and HCC tissue samples. Our data showed that miR-491 had a negative relationship with CSCs-like properties both in cell lines and tissue samples of HCC. Further, miR-491 levels of non-recurrence HCC tissues were higher than those of recurrence HCC tissues. In HCC cell lines, nuclear factor kappa B (NF-κB)/snail pathway was involved in the epithelial to mesenchymal transition and the maintenance of CSCs-like properties. Overexpression of miR-491 targeted G-protein-coupled receptor kinase-interacting protein 1 (GIT-1), which blocked the activation of NF-κB by the inhibition of extracellular signal-regulated kinases (ERKs). Such process attenuated the CSCs-like properties in HCC cells. Our results point to a previously undefined mechanism by which miR-491 decreases CSCs-like properties and help to identify potential targets for the therapy of HCCs.

Keywords Hepatocellular carcinoma · Cancer stem cells-like properties · Epithelial to mesenchymal transition · microRNA-491 · G-protein-coupled receptor kinase-interacting protein 1 · Nuclear factor kappa B

Introduction

Hepatocellular carcinoma (HCC) is the sixth highest incidence of cancer and the third highest cause of cancer death worldwide [1]. Intrahepatic and extrahepatic metastasis and postsurgical recurrence lead to poor prognosis for HCC patients [2]. Current standard treatments such as surgical resection and liver transplantation for HCC patients are less than satisfactory as high postsurgical recurrence rates [3, 4]. Researches have been made to discuss molecular factors correlating with the prognosis for HCC patients; however, the molecular pathogenesis underlying metastasis and recurrence remains obscure. Our previous report showed that microRNA-491 (miR-491) inhibits metastasis of HCCs through the inhibition of epithelial to mesenchymal transition (EMT) process, but a continued search for links between miR-491 and the EMT of HCC is essential [5].

A brand new conception proposed to explain the characteristics of neoplastic tissues is the existence of self-renewing, stem-like cells, called cancer stem cells (CSCs) [6]. CSCs have been identified in lung cancer [7], breast cancer [8], glioblastoma [9], colorectal cancer [10], and HCC [11]. CSCs

Xiaojun Yang, Jing Ye, and Han Yan contributed equally to this work.

Electronic supplementary material The online version of this article (doi:10.1007/s13277-015-3687-5) contains supplementary material, which is available to authorized users.

✉ Jianping Zhang
drjpzhang@hotmail.com

✉ Lihua Yang
njmuyanglihua@hotmail.com

[1] Department of General Surgery, The Second Affiliated Hospital, Nanjing Medical University, 121 Jiang Jiayuan, Nanjing 210029, Jiangsu, China

[2] Department of Gastroenterology, The Second Affiliated Hospital, Nanjing Medical University, 121 Jiang Jiayuan, Nanjing210029Jiangsu, China

are defined by their capacity to regenerate new tumors which constitute only a small portion of the neoplastic cells within a tumor. On this account, they are also termed *tumor initiating cells*. Close relationships have been proven between the EMT and CSCs in that EMT cells acquire CSCs-like traits as well as mesenchymal-like appearance of CSCs [12]. We assume that associations between EMT and induction of CSCs may clarify the mechanism of EMT-induced tumor metastasis and post-surgical recurrence.

We previously reported that, as determined by a high-throughput miRNA microarray, 41 miRNAs are differentially expressed in HCC tissues with different statuses of differentiation. Among these, miR-491 levels are extensively downregulated in poorly differentiated HCC tissues relative to well-differentiated HCC tissues [5]. The present study aimed to investigate the action of miR-491 on the EMT progression, and the molecular mechanisms underlying in, which are responsible for CSCs-like properties and recurrence of HCCs, in cell lines and tissues with different potentials for metastasis.

Materials and methods

Patients and tissue specimens

This study was reviewed and approved by the Medical Ethics Committee of Nanjing Medical University. The approbation of our ethics committees and the participants' written informed consent were listed in the supporting information. A cohort of 92 Chinese HCC patients was enrolled in this study. These patients underwent curative liver resection for primary tumors between May 2009 and Mar 2012 at The Second Affiliated Hospital of Nanjing Medical University (n=32) and The First Affiliated Hospital of Nanjing Medical University (n=60). The inclusion criteria of the cohort included (i) having a distinctive pathologic diagnosis of HCC; (ii) undergoing surgical resection, defined as complete resection of all tumor nodules with the cut margin being free of cancer by histologic examination; and (iii) having complete clinicopathologic data. An exclusion criterion was prior anticancer treatment before liver resection. None of the patients had extrahepatic metastases when they underwent hepatectomies. The clinicopathologic characteristics of the patients are shown in Table 1.

Table 1 The detailed characteristics of the patients with different status of differentiation in HCC tissues

Characteristic	Well differentiated n=33	Poorly differentiated n=59
Age (years)		
≤50	19	34
>50	14	25
Gender		
Male	27	40
Female	6	19
HBsAg		
Positive	27	50
Negative	6	9
Serum AFP (ng/ml)		
≤200	9	10
>200	24	49
Liver cirrhosis		
Yes	27	44
No	6	15
Tumor size		
≤3 cm	23	31
>3 cm	10	28
Multinodular tumor		
Yes	20	25
No	13	34
BCLC stage		
0/A	9	19
B	24	40

Cell culture and reagents

MHCC97H and MHCC97L cells (HCC cell lines with high and low migratory potential, respectively) were obtained from the Liver Cancer Institute, Zhongshan Hospital, Fudan University, Shanghai, China. They have the same genetic backgrounds, without cross contaminating with another cell line, and are widely applied in the study of HCC metastasis in vitro [5, 13]. HepG2 cells (an HCC cell line with low migratory capacity), were obtained from the Shanghai Institute of Cell Biology, Chinese Academy of Sciences (Shanghai, China). Cells were maintained in 5 % CO_2 at 37 °C in Dulbecco's Modified Eagle Medium (DMEM, Life Technologies/Gibco, Grand Island, NY) supplemented with 10 % fetal bovine serum (FBS, Life Technologies/Gibco), 100 U/ml penicillin, and 100 μg/ml streptomycin (Life Technologies/Gibco, Gaithersburg, MD). A mycoplasma stain assay Kit (Beyotime, Haimeng, China) was used for mycoplasma testing to rule out the possibility of cryptic contamination. All the other reagents used were of analytical grade or the highest grade available.

Quantitative real-time polymerase chain reaction

Total cellular RNA was isolated by use of Trizol (Invitrogen, Carlsbad, CA, USA) according to the manufacturer's recommendations. For detection of CD44, CD90, EpCAM, and snail, total RNA (2 μg) was transcribed into cDNA by use of AMV Reverse Transcriptase (Promega, Madison, Wisconsin, USA). Quantitative real-time polymerase chain reaction (qRT-PCR) was performed using the Applied Biosystems

7300HT machine and MaximaTM SYBR Green/ROX qPCR Master Mix (Fermentas, Waltham, MA, USA). The PCR reaction was evaluated using melting curve analysis. Glyceraldehyde 3-phosphate dehydrogenase (GAPDH) was amplified to ensure cDNA integrity and to normalize expression. For detection of mature miR-491, 2 μg of total RNA, miR-491-specific stem-loop RT primers, and MMLV reverse transcriptase (Promega) were used in reverse transcription following the manufacturer's protocol. The sequences of mature miR-491 were from Sanger miRBase (http://microrna.sanger.ac.uk/sequences/). qRT-PCR was performed using the Power SYBR Green Master Mix (Applied Biosystems, Foster City, CA, USA) and an ABI 7300 real-time PCR detection system (Applied Biosystems). The U6snRNA was used as an internal control. Fold changes in expression of each gene were calculated by a comparative threshold cycle (Ct) method using the formula $2-(\Delta\Delta Ct)$. The primers used were listed in Table 2.

Spheroid formation

In non-adherent dishes (Costar, Cole-Parmer, Vernon Hills, IL), cells (1×104) were suspended in defined, serum-free medium composed of DMEM/F-12 (Gibco), 10 ng/mL of human recombinant basic fibroblast growth factor (bFGF, R&D Systems, Minneapolis, MN), and 10 ng/mL of epidermal growth factor (EGF, R&D Systems). Cells were grown for 10 days and fed every 48 h. Total spheres were then counted under a microscope (Olympus, Tokyo, Japan).

Cell transfection

Anti-con, anti-miR-491, con-mimic, and miR-491-mimic were synthesized by RiBoBio Co. Cells were transiently transfected using the Lipofectamine 2000 reagent (Invitrogen), according to the manufacturer's protocol. For miR-491 inhibition, cells were seeded in six-well plates at a density of 1×105 per well. After 48 h, these cells were transfected with 100 nM of anti-miR-491 or anti-con for 12 h. For miR-491 overexpression, cells were seeded in six-well plates at a density of 1×105 per well. After 48 h, these cells were transfected with 50 nM of miR-491-mimic or con-mimic for 12 h. After transfection, cells were cultured in fresh DMEM medium supplemented with 10 % FBS (Gibco), 100 U/ml penicillin, and 100 μg/ml streptomycin (Gibco) for another 24 h before being used for other experiments.

Western blots

Cells were washed twice with ice-cold PBS and then scraped off in 0.2 mL of buffer (20 mM HEPES, pH 6.8; 5 mM EDTA; 10 mM EGTA; 5 mMNaF; 0.1 μg/mL okadaic acid; 1 mM DTT; 0.4 M KCl; 0.4 % Triton X-100; 10 % glycerol; 5 μg/mL leupeptin; 50 μg/mL PMSF; 1 mMbenzamidine; 5 mg/mL aprotinin; 1 mM Na orthovanadate) and incubated on ice for 30 min, followed by centrifugation at 12,000 rpm for 15 min. Protein concentrations were measured with the BCA protein assay (Pierce, Rockford, IL, USA). Afterwards, proteins were diluted to equal concentrations (20 μg), boiled for 5 min, and separated by 10 % sodium dodecyl sulfate (SDS)-polyacrylamide gel electrophoresis. Then the proteins were transferred to polyvinylidene fluoride (PVDF) membranes (Millipore, Billerica, USA), which were probed with primary antibody (dilutions, 1:500) overnight at 4 °C. Antibodies used were E-cadherin, vimentin, p65, p-p65 (ser536), ERKs, p-ERKs (Thr202/Tyr204), and snail (Cell Signaling Technology); GIT-1 and GAPDH, Sigma. Then, membranes were incubated with horseradish peroxidase-conjugated secondary antibodies (Beyotime) for 1 h at room temperature (RT) to enhance chemiluminescence before exposure to film. GAPDH was used to normalize for protein loading.

Luciferase reporter assay

The pGL3-GIT-1 3′UTR (wide type, wt)-Luc construct and the pGL3-GIT-1 3′UTR (mutation, mt)-Luc construct were purchased from Shuntian Biology (Shanghai). The plasmid phRL-tk (used as internal control for transfection efficiency and cytotoxicity of test chemicals) containing the Renilla luciferase gene was purchased from Promega (Madison, WI, USA). Briefly, cells were plated in 100-mm cell culture dishes. The cells proliferated to 60 to 80 % confluence after 24 h of culture. MiR-491 mimics or miR-491 inhibitor was co-transfected with the reporter constructs, respectively, by using Lipofecamine 2000 reagent (Invitrogen, Carlsbad, CA) according to the manufacturer's protocol. After an incubation period of 12 h, the transfection medium was replaced. Then the cells were harvested and washed with PBS (pH 7.4). The cells were lysed with passive lysis buffer (Promega). The cell lysates were analyzed immediately with a 96-well plate luminometer (Berthold Detection System, Pforzheim, Germany). The amounts of luciferase and Renilla luciferase were measured with the Dual-Luciferase Reporter Assay System Kit (Promega) following the manufacturer's instructions. The values of luciferase activity for each lysate were normalized to the Renilla luciferase activity. The relative transcriptional activity was converted into fold induction above the vehicle control value.

Southwestern analyses

Southwestern analyses were performed as described previously [14]. Briefly, the nuclear extracts (80 μg) were separated by SDS-PAGE and transferred to nitrocellulose membranes (Millipore). After the transfer, the filters were hybridized for 2 h at 20 °C with binding buffer containing 40 ng of the biotin-labeled probe (κB: GGGGGTTTCC). The positions of the

Table 2 Primers used for qRT-PCR

Genes	Primers (5′-3′)
CD44	TGAGCATCGGATTTGAGAC (F)
	CATACTGGGAGGTGTTGGA (R)
CD90	AAGGAGAAACAGGAAACCTC (F)
	ACAGACACAGTCCAACTTCC (R)
EpCAM	AAGGAGAAACAGGAAACCTC (F)
	ACAGACACAGTCCAACTTCC (R)
Snail	TTCTCCCGAATGTCCCT (F)
	TCAGCCTTTGTCCTGTAGC (R)
miR-491 (for RT)	CTCAACTGGTGTCGTGGAGTCGGCAATTCAGTTGAGCCTCATGG
miR-491 (for qPCR)	ACACTCCAGCTGGGAGTGGGGAACCCTTCC (F)
	TGGTGTCGTGGAGTCG (R)
U6 (for RT)	AAAATATGGAACGCTTCACG
U6 (for qPCR)	CGCTTCGGCAGCACATATACTAAAATTGGAAC (F)
	GCTTCACGAATTTGCGTGTCATCCTTGC (R)

biotin end-labeled oligonucleotides were detected by a chemiluminescent reaction according to the manufacturer's instructions (Pierce, Rockford, USA) and visualized by autoradiography.

Statistical analysis

Derived values were presented as the means±SD. A Student's *t* test, and a one-way analysis of variance (ANOVA) followed by Dunnett's *t* test were used to assess significant differences between groups. *P* values <0.05 were considered statistically significant.

Results

Expressions of miR-491 and CSCs-like markers are associated with malignant behavior of cell lines and tissue samples of HCC

Our previous study showed that miR-491 expression was downregulated in 17 poorly differentiated HCC tissues [5]. Here, we continuously verified that the expression of miR-491 was downregulated in the poorly differentiated group in 92 HCC tissues (Fig. 1a). CD44, CD90, and EpCAM are representative cell-surface markers of CSCs-like cells in HCC [15]. We then used qRT-PCR to determine the expressions of CSCs-like surface markers in these HCC tissues. As shown in Figs. 1b, c, expressions of CD44, CD90, and EpCAM mRNA in poorly differentiated HCCs were higher than those in well-differentiated HCCs.

Next, we used three HCC cell lines HepG2, MHCC97L, and MHCC97H (our previous study showed that the migration potential, HepG2<MHCC97L<MHCC97H [5]) to specify the relationship between miR-491 and CSCs-like properties in HCC. High rates of migratory behavior of HCC cell lines were prone to have a lower expression of miR-491 (Fig. 1d), and more elevation of CSCs-like properties as determined by CSCs-like markers (Fig. 1e) and formation of spheroids, which represented the capacity for self-renewal [16] (Fig. 1f, g). These results indicate that miR-491 has a negative relationship with CSCs-like properties both in cell lines and tissue samples of HCC.

MiR-491 attenuates the CSCs-like properties in HCC cells

We then investigated the functions of miR-491 on CSCs-like properties in HCC cell lines. Compared with HepG2 cells, there was relative lower background expression of miR-491 in MHCC97H cells. Here, overexpression of miR-491 (Fig. 2a) decreased the expressions of CD44, CD90, EpCAM (Figs. 2b, c), and attenuated the capacity for formation of spheroids (Fig. 2d). Further, in HepG2 cells, knockdown of miR-491 (Fig. 2e) improved the expressions of CD44, CD90, EpCAM (Figs. 2f, g), and elevated the capacity for formation of spheroids (Fig. 2h). These results suggest that miR-491 attenuates the CSCs-like properties in HCC cells.

NF-κB is involved in the maintenance of CSCs-like properties of HCC cells and is associated with malignant behavior in HCC tissue samples.

We previously showed that NF-κB is involved in the acquirement of EMT and CSCs-like properties by the activation of snail [16]. Here, as shown in Fig. 3a, activation of NF-κB (as determined by the phosphorylation of NF-κB/p65), the expression of vimentin (a mesenchymal marker), and snail in poorly differentiated HCCs was

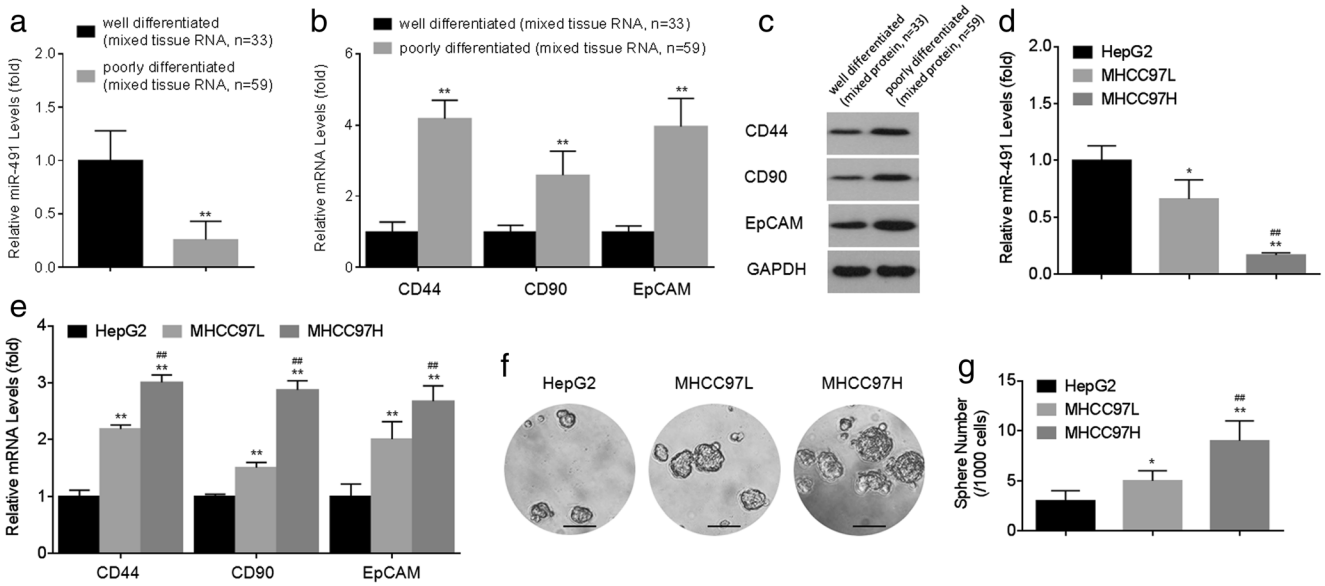

Fig. 1 Expressions of miR-491 and CSCs-like markers are associated with malignant behavior of cell lines and tissue samples of HCC. **a** and **b** qRT-PCR analyses of miR-491, CD44, CD90, and EPCAM levels in HCC tissues with different statuses of differentiation, $^{**}p<0.01$ compared with well-differentiated group. **c** Western blot analyses of the expressions of CD44, CD90, and EpCAM proteins. **d** and **e** qRT-PCR analyses of miR-491, CD44, CD90, and EPCAM levels in HCC cells. **f** Free-floating, viable spheres formed by HCC cells (*bars* 125 μm). **g** Sphere quantitation.$^{*}p<0.05$ and $^{**}p<0.01$ compared with HepG2 cells; $^{\#\#}p<0.01$ compared with MHCC97L cells

higher than those in well-differentiated HCC tissues; while the expression of E-cadherin (an epithelium marker) was lower than that in well-differentiated tissues. In HCC cell lines, we also found that, with more migration behavior of HCC cells, there was more increased phosphorylation of NF-κB/p65 (Fig. 3b).

Then, we used a specific siRNA to knockdown NF-κB for further investigating the effects of NF-κB on CSCs-like properties in HCC cells. As MHCC97H cells exhibited a spindle-like mesenchymal morphology [5], we firstly determined the functions of NF-κB on the EMT process in MHCC97H cells. Our data showed that

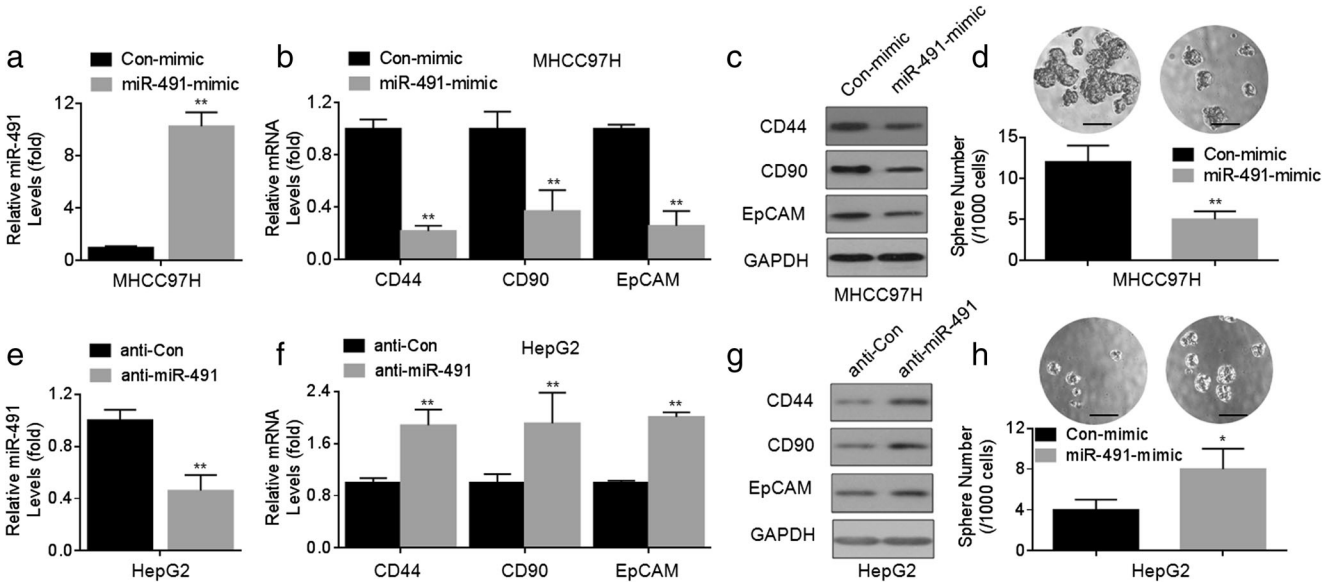

Fig. 2 MiR-491 attenuates the CSCs-like properties in HCC cells. **a**–**d** MHCC97H cells were transfected by con-mimic or miR-491 mimic for 12 h. **a** and **b** qRT-PCR analyses of miR-491, CD44, CD90, and EPCAM levels in MHCC97H cells. **c** Western blots analyses of CD44, CD90, and EPCAM levels in MHCC97H cells. **d**, *top* Free-floating, viable spheres formed by HCC cells (*bars* 125 μm), *bottom* Sphere quantitation. $^{**}p<0.01$ compared with MHCC97H cells transfected by con-mimic. **e**–**h** HepG2 cells were transfected by anti-con or anti-miR-491 for 12 h. **e** and **f** qRT-PCR analyses of miR-491, CD44, CD90, and EPCAM levels in HepG2 cells. **g** Western blots analyses of CD44, CD90, and EPCAM levels in HepG2 cells. **h**, *top* Free-floating, viable spheres formed by HCC cells (*bars* 125 μm), *bottom* Sphere quantitation. $^{*}p<0.05$ and $^{**}p<0.01$ compared with HepG2 cells transfected by anti-con

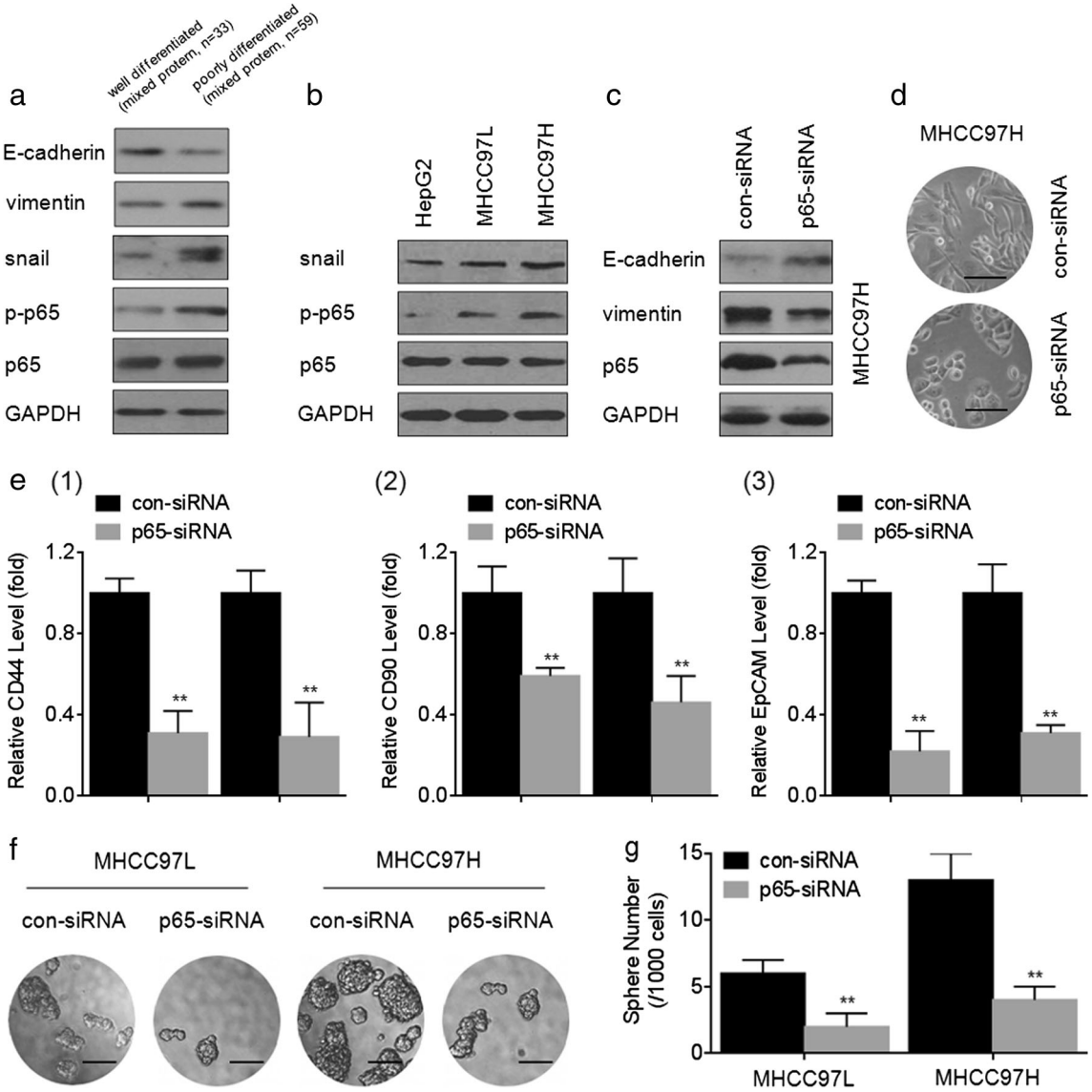

Fig. 3 NF-κB is involved in the maintenance of CSCs-like properties of HCC cells and is associated with malignant behavior in HCC tissue samples. Western blots analyses of E-cadherin, vimentin, snail, p-p65, and p65 levels in HCC tissues with different statuses of differentiation (**a**) and in HCC cells (**b**). **c**–**e** MHCC97H cells were transfected by 10 nM of con-siRNA or p65-siRNA for 12 h. **c** Western blots analyses of E-cadherin, vimentin, and p65 levels. **d** Cell morphology. **e** qRT-PCR analyses of CD44, CD90, and EPCAM levels. **f** and **g** MHCC97L and MHCC97H cells were transfected by 10 nM of con-siRNA or p65-siRNA for 12 h, respectively. **f** Free-floating, viable spheres formed by HCC cells (*bars* 125 μm), **g** Sphere quantitation. $^{**}p<0.01$ compared with cells transfected by con-siRNA

knockdown of NF-κB improved the expression of E-cadherin but decreased the expression of vimentin, and changed the cell morphology to an epithelial-like properties (Figs. 3c, d). Then, we further investigated the effects of NF-κB on CSCs-like properties in both MHCC97L and MHCC97H cells. Here, knockdown of NF-κB decreased the expressions of CD44, CD90, and EpCAM (Fig. 3e), and attenuated the capacity for formation of spheroids (Figs. 3f, g). Collectively, these data suggest that the NF-κB may be involved in the maintenance of CSCs-like properties in HCC cell lines and tissue samples.

MiR-491 blocks the activation of NF-κB/snail signal pathway by GIT-1-mediated ERKs inactivation

We then determined the effects of miR-491 on the signal pathway of NF-κB. Compared with HepG2 cells, there was relative lower background expression of miR-491 and higher background activation (phosphorylation) of NF-κB in MHCC97H cells. We firstly used miR-491-mimc to improve the expression of miR-491. As shown in Figs. 4a, b, overexpression of miR-491 decreased the levels of p-p65 and snail. Meanwhile, southwestern assay suggested that miR-491 attenuated the DNA-binding

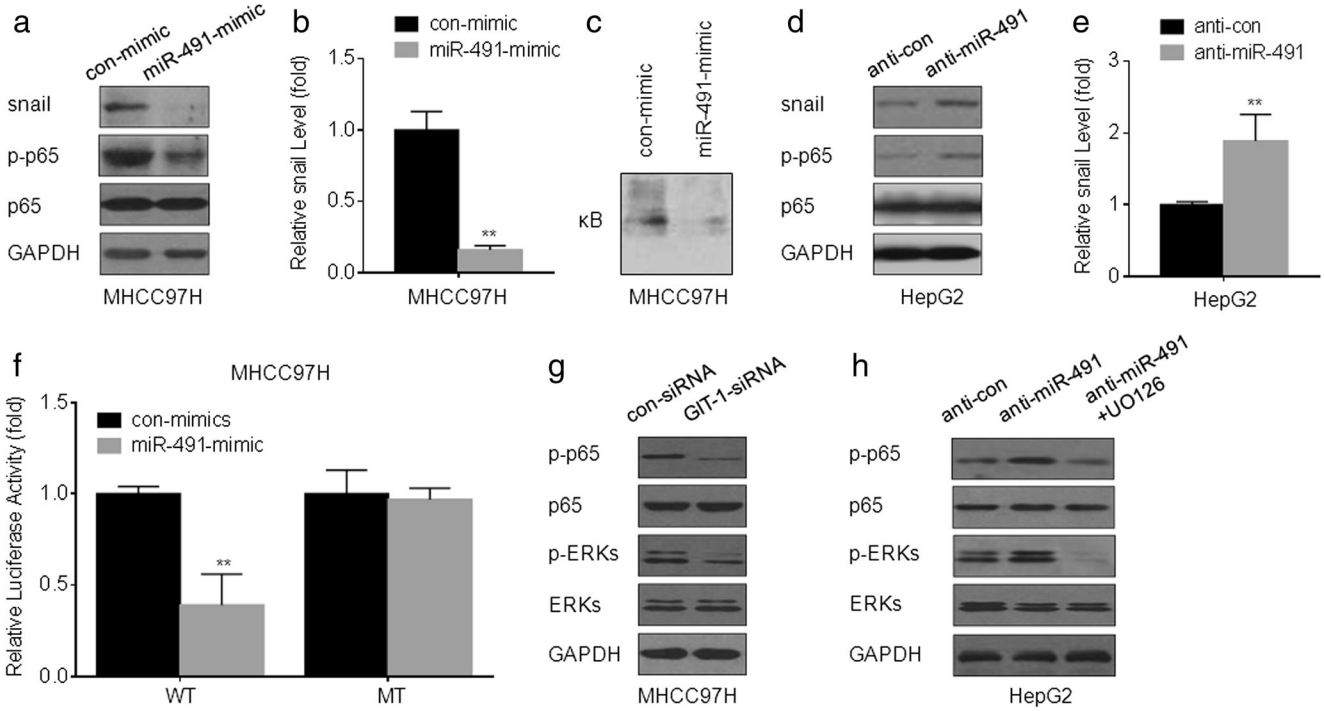

Fig. 4 MiR-491 blocks the activation of NF-κB/snail signal pathway. **a**–**c** MHCC97H cells were transfected by con-mimic or miR-491 mimic for 12 h. **a** Western blots analyses of snail, p-p65, and p65 levels. **b** qRT-PCR analyses of snail level. **c** Southwestern blots analyses the binding of NF-κB to DNA (κB: GGGGGTTTCC). $^{**}p<0.01$ compared with MHCC97H cells transfected by con-mimic. **d** and **e** HepG2 cells were transfected by anti-con or anti-miR-491 for 12 h. **d** Western blots analyses of snail, p-p65, and p65 levels. **e** qRT-PCR analyses of snail level. $^{**}p<0.01$ compared with HepG2 cells transfected by anti-con

activity of NF-κB (Fig. 4c). Then we used HepG2 cells to further confirm our conclusion. As shown in Fig. 4d, e, knockdown of miR-491 improved the expressions of p-p65 and snail. These results indicate that miR-491 blocks the activation of NF-κB/snail signal pathway in HCC cells.

We further determined the upstream regulator involved in the miR-491-mediated inhibition of NF-κB. Recent study suggests that the G-protein-coupled receptor kinase-interacting protein 1 (GIT1), a ERKs activator, is a direct target gene controlled by miR-491 in oral squamous cell carcinoma [17–20]. Here, to verify whether miR-491 directly targeted GIT-1 in HCC cell lines, luciferase reporter assays were conducted. In MHCC97H, co-transfected with pGL3-GIT-1 3′UTR (wt)-Luc construct and miR-491-mimic caused a significant decrease in the luciferase activity (Fig. 4f). We previously demonstrated that ERKs was an upstream regulator, which activated NF-κB 26. Here, knockdown of GIT-1 decreased the phosphorylation of p-ERKs and p65 (Fig. 4g). Furthermore, in HepG2 cells, knockdown of miR-491 improved the activation of ERKs and NF-κB, however, inhibition of ERKs blocked such phenomenon (Fig. 4h). Collectively, these results suggest that miR-491 blocks the activation of NF-κB/snail signal pathway by GIT-1-mediated ERKs inactivation.

MiR-491 is inversely correlated with recurrence in HCC patients

We conducted a long-term follow-up work for overall 92 post-surgical HCC patients. Data showed that the recurrence rate (38/59) in poorly differentiated HCC patients was obviously higher than that (9/33) in well-differentiated HCC patients, which demonstrates that the outcome of poorly differentiated HCC patients is poorer than that of well-differentiated HCC patients. After that, we re-divided the HCC tissue specimens (the initial tissue samples taken during surgical removal of tumors) into both non-recurrence and recurrence groups, and re-determined the expressions of miR-491 and CSCs-like markers. The expression of miR-491 was downregulated in the recurrence group (Fig. 5a) while the expressions of CD44, CD90, and EpCAM in recurrence group were higher than the level in non-recurrence group (Figs. 5b, c). These results prompt that miR-491 is inversely correlated with the CSCs-like properties and the probability of recurrence in HCC patients.

Discussion

HCC has represented the sixth most common cancer for years worldwide as well as being the third leading cause of cancer

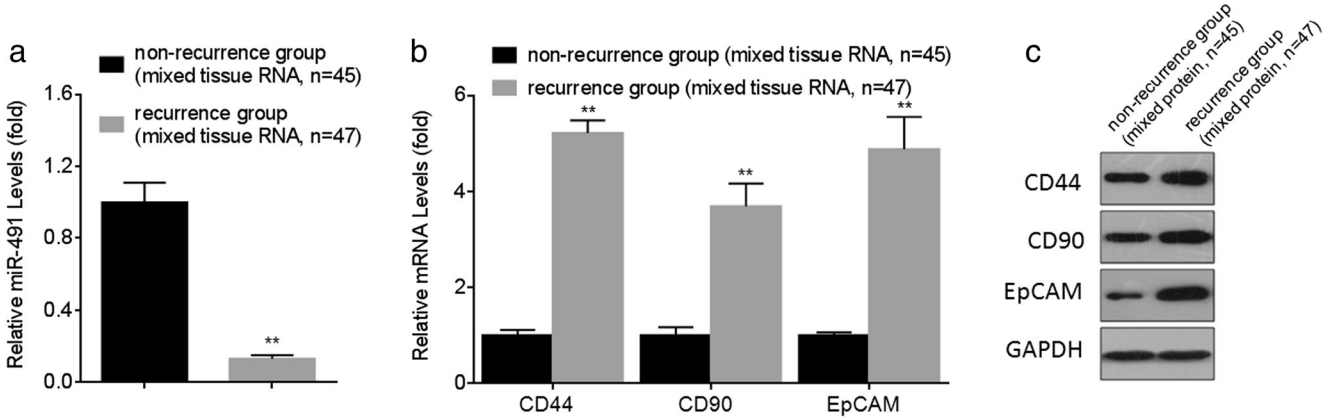

Fig. 5 MiR-491 is inversely correlated with recurrence in HCC patients. **a** and **b** qRT-PCR analyses of miR-491, CD44, CD90, and EPCAM levels in HCC tissues with different outcome (recurrence or no-recurrence), $^{**}p<0.01$ compared with no-recurrence group. **c** Western blots analyses of CD44, CD90, and EPCAM levels in HCC tissues with different outcome (recurrence or no-recurrence)

related death. Surgical resection and liver transplantation still stands for the primary treatment guidelines for HCC. Despite molecular biological and the clinical advances, high-frequency postsurgical recurrence constrains the development of prognosis for HCC [1, 2]. Current chemotherapy against HCC usually aims at the bulk population of tumor cells directly, which successfully shrinks the primary tumor but fails to eradicate the lesions consistently [3, 4]. The discovery among the ideas of CSCs has renovated our view of carcinogenesis and chemotherapy. CSCs, also termed *tumor initiating cells*, underline the capacity to form new metastasis tumors, CSCs are critical to the formation and growth of neoplastic tissue and the resistance to chemotherapeutic agents, which discloses why traditional drugs can initially shrink a tumor but fail to eradicate it, leading to the ultimate recurrence [21]. Therefore, a continuous research for the molecular markers that target HCC cells with CSCs-like properties is indispensible. As we reported previously, miR-491 is involved in metastasis of HCC by inhibition of MMPs and the EMT. Here, we further found that miR-491 could attenuate the CSCs-like properties and inversely correlated with the recurrence of HCC.

The EMT features a loss of epithelial properties, such as cell adhesion; low expression of the epithelial marker, E-cadherin; and acquisition of mesenchymal properties, such as increased cell motility and expression of the mesenchymal marker, vimentin. It is involved in the development of embryogenesis [22]. In the case of cancer, similar cell transformations are recapitulated during its pathological processes. Most of the research conducted on the EMT process has concentrated on the morphology of the invasion and metastasis of cancer cells. Particularly, there is a relationship between the EMT and CSCs in that stem cell-like traits enable EMT processes while CSCs display a mesenchymal-like appearance. The link between EMT and induction of CSCs may account for why EMT induces the initiation and progression of neoplasm. Several developmental genes that induce EMT act as E-cadherin repressors such as snail, slug, and twist1/2 [23, 24]. The first among these is zinc-finger transcriptional factors from snail family that bind DNA by recognizing E-box motifs in target promoters like E-cadherin [25]. The initiation and maintenance of EMT process embodies a variety of signal pathways. Our previous study demonstrated that miR-491 inhibits EMT in HCC cell lines and in HCC tissues. In this report, we further found that such process might be mediated by the inhibition of NF-κB/snail signal pathway.

NF-κB signaling pathway is involved in cancer development and progression. Inhibition of NF-κB restrains the cell transformation induced by tumor promoters [16]. Snail functions as a regulator to suppress the expression of adhesion molecules and to assist the escape of tumor cells from cell death during EMT. NF-κB binds to the snail promoter and transcriptionally upregulates snail expression [16, 25]. As shown in the present study, overexpression of miR-491 inhibits NF-κB and snail expression in MHCC97H cells. However, in HepG2 cells, knockdown of miR-491 blocks NF-κB/snail signaling. Further, in our present study, miR-491 inhibited phosphonation of p65, but the expression of p65 was not affected, suggesting the indirect activation of miR-491 on p65 activation. Recent study suggests that the G-protein-coupled receptor kinase-interacting protein 1 (GIT1) is a direct target gene controlled by miR-491 [17]. Overexpression of GIT1 abolishes the miR-491-mediated inhibition of cancer metastasis [17]. Moreover, GIT1 binds to extracellular signal-regulated kinases (ERKs), which activates ERKs in response to epidermal growth factor [18, 19]; further, GIT1 activates ERKs to induce growth in human liver and colon cancer [20]. We and other groups previously showed that ERKs upregulated the activation of NF-κB [26–28]. Here, we suggested that the direct target of miR-491 on upstream of NF-κB pathway was the GIT1-mediated ERKs activation.

In sum, in HCC cells and tissue samples, miR-491 decreases activation of the NF-κB/snail signal pathway by GIT-1 mediated ERKs inactivation. Such process blocks the EMT process. Such progression attenuates the CSC-like properties in HCC cells. The results help to identify potential targets for the therapy of HCC.

Acknowledgments The authors wish to thank Donald L. Hill (University of Alabama at Birmingham, USA) for editing. This work was supported by the Natural Science Foundations of China (81272713, 81100253, and 81273114).

Conflicts of interest The authors declare they have no competing financial interests. The funders had no role in study design, data collection and analysis, decision to publish, or preparation of the manuscript.

References

1. Tsochatzis EA, Meyer T, Burroughs AK. Hepatocellular carcinoma. N Engl J Med. 2012;366:92–3.
2. Thomas MB, Jaffe D, Choti MM, Belghiti J, Curley S, Fong Y, et al. Hepatocellular carcinoma: consensus recommendations of the national cancer institute clinical trials planning meeting. J Clin Oncol Off J Am Soc Clin Oncol. 2010;28:3994–4005.
3. Farazi PA, DePinho RA. Hepatocellular carcinoma pathogenesis: from genes to environment. Nat Rev Cancer. 2006;6:674–87.
4. Uchino K, Tateishi R, Shiina S, Kanda M, Masuzaki R, Kondo Y, et al. Hepatocellular carcinoma with extrahepatic metastasis: clinical features and prognostic factors. Cancer. 2011;117:4475–83.
5. Zhou Y, Li Y, Ye J, Jiang R, Yan H, Yang X, et al. Microrna-491 is involved in metastasis of hepatocellular carcinoma by inhibitions of matrix metalloproteinase and epithelial to mesenchymal transition. Liver Int Off J Int Assoc Study Liver. 2013;33:1271–80.
6. Garcion E, Naveilhan P, Berger F, Wion D. Cancer stem cells: beyond Koch's postulates. Cancer Lett. 2009;278:3–8.
7. Xin YH, Bian BS, Yang XJ, Cui W, Cui HJ, Cui YH, et al. Pou5f1 enhances the invasiveness of cancer stem-like cells in lung adenocarcinoma by upregulation of mmp-2 expression. PLoS One. 2013;8, e83373.
8. Avivar-Valderas A, Wen HC, Aguirre-Ghiso JA: Stress signaling and the shaping of the mammary tissue in development and cancer. Oncogene. 2014
9. Jun HJ, Bronson RT, Charest A. Inhibition of egfr induces a c-met-driven stem cell population in glioblastoma. Stem Cells. 2014;32:338–48.
10. Hirsch D, Barker N, McNeil N, Hu Y, Camps J, McKinnon K, et al. Lgr5 positivity defines stem-like cells in colorectal cancer. Carcinogenesis. 2014;35:849–58.
11. Kim HM, Haraguchi N, Ishii H, Ohkuma M, Okano M, Mimori K, et al. Increased cd13 expression reduces reactive oxygen species, promoting survival of liver cancer stem cells via an epithelial-mesenchymal transition-like phenomenon. Ann Surg Oncol. 2012;19 Suppl 3:S539–548.
12. Mani SA, Guo W, Liao MJ, Eaton EN, Ayyanan A, Zhou AY, et al. The epithelial-mesenchymal transition generates cells with properties of stem cells. Cell. 2008;133:704–15.
13. Ding SJ, Li Y, Shao XX, Zhou H, Zeng R, Tang ZY, et al. Proteome analysis of hepatocellular carcinoma cell strains, mhcc97-h and mhcc97-l, with different metastasis potentials. Proteomics. 2004;4:982–94.
14. Li Y, Ling M, Xu Y, Wang S, Li Z, Zhou J, et al. The repressive effect of nf- b on p53 by mot-2 is involved in human keratinocyte transformation induced by low levels of arsenite. Toxicol Sci. 2010;116:174–82.
15. Yamashita T, Honda M, Nakamoto Y, Baba M, Nio K, Hara Y, et al. Discrete nature of epcam+and cd90+ cancer stem cells in human hepatocellular carcinoma. Hepatology. 2013;57:1484–97.
16. Jiang R, Li Y, Xu Y, Zhou Y, Pang Y, Shen L, et al. Emt and csc-like properties mediated by the ikkbeta/ikappabalpha/rela signal pathway via the transcriptional regulator, snail, are involved in the arsenite-induced neoplastic transformation of human keratinocytes. Arch Toxicol. 2013;87:991–1000.
17. Huang WC, Chan SH, Jang TH, Chang JW, Ko YC, Yen TC, et al. Mirna-491-5p and git1 serve as modulators and biomarkers for oral squamous cell carcinoma invasion and metastasis. Cancer Res. 2014;74:751–64.
18. Yin G, Haendeler J, Yan C, Berk BC. Git1 functions as a scaffold for mek1-extracellular signal-regulated kinase 1 and 2 activation by angiotensin ii and epidermal growth factor. Mol Cell Biol. 2003;24:875–85.
19. Zhang N, Cai W, Yin G, Nagel DJ, Berk BC. Git1 is a novel mek1-erk1/2 scaffold that localizes to focal adhesions. Cell Biol Int. 2010;34:41–7.
20. Peng H, Dara L, Li TW, Zheng Y, Yang H, Tomasi ML, et al. Mat2b-git1 interplay activates mek1/erk 1 and 2 to induce growth in human liver and colon cancer. Hepatology. 2013;57:2299–313.
21. Yan H, Dong X, Zhong X, Ye J, Zhou Y, Yang X, Shen J, Zhang J. Inhibitions of epithelial to mesenchymal transition and cancer stem cells-like properties are involved in mir-148a-mediated anti-metastasis of hepatocellular carcinoma. Mol Carcinog. 2013
22. Kalluri R, Weinberg RA. The basics of epithelial-mesenchymal transition. J Clin Invest. 2009;119:1420–8.
23. Zhang K, Zhaos J, Liu X, Yan B, Chen D, Gao Y, et al. Activation of nf-b upregulates snail and consequent repression of e-cadherin in cholangiocarcinoma cell invasion. Hepatogastroenterology. 2011;58:1–7.
24. Lee TK, Poon RT, Yuen AP, Ling MT, Kwok WK, Wang XH, et al. Twist overexpression correlates with hepatocellular carcinoma metastasis through induction of epithelial-mesenchymal transition. Clin Cancer Res Off J Am Assoc Cancer Res. 2006;12:5369–76.
25. Zhu LF, Hu Y, Yang CC, Xu XH, Ning TY, Wang ZL, et al. Snail overexpression induces an epithelial to mesenchymal transition and cancer stem cell-like properties in scc9 cells. Laboratory investigation. J Tech Methods Pathol. 2012;92:744–52.
26. Li Y, Jiang R, Zhao Y, Xu Y, Ling M, Pang Y, et al. Opposed arsenite-mediated regulation of p53-survivin is involved in neoplastic transformation, DNA damage, or apoptosis in human keratinocytes. Toxicology. 2012;300:121–31.
27. Kim JH, Na HK, Pak YK, Lee YS, Lee SJ, Moon A, et al. Roles of erk and p38 mitogen-activated protein kinases in phorbol ester-induced nf-kappab activation and cox-2 expression in human breast epithelial cells. Chem Biol Interact. 2008;171:133–41.
28. Kavitha K, Kowshik J, Kishore TK, Baba AB, Nagini S. Astaxanthin inhibits nf-kappab and wnt/beta-catenin signaling pathways via inactivation of erk/mapk and pi3k/akt to induce intrinsic apoptosis in a hamster model of oral cancer. Biochim Biophys. 1830;2013:4433–44.